

UKAEA FUS 426

EURATOM/UKAEA Fusion

**A rotating shell and stabilisation of the
tokamak resistive wall mode**

C Gimblett and R J Hastie

April 2000

© UKAEA

EURATOM/UKAEA Fusion Association

Culham Science Centre, Abingdon
Oxfordshire, OX14 3DB
United Kingdom
Telephone +44 1235 463311
Facsimile +44 1235 463647

A Rotating Shell and Stabilisation of the Tokamak Resistive Wall Mode

C. G. Gimblett and R. J. Hastie*

*EURATOM/UKAEA Fusion Association, Culham Science Centre
Abingdon, Oxon, OX 14 3DB, United Kingdom*

**Current address: MIT Plasma Science & Fusion Centre, 167 Albany
Street, NW16-234 Cambridge, MA 02139, USA*

Abstract

The finite resistivity of the wall that surrounds any toroidal plasma confinement device can lead to a branch of instabilities known as the Resistive Wall Mode (RWM). Theory indicates that the RWM is potentially activated whenever the plasma equilibrium is unstable with the wall placed at infinity. In particular, Advanced Tokamak power plant designs require the plasma β to be above the critical value for this condition to be satisfied. Accordingly, it is important to find a method of stabilising this mode. In this work we describe a method of stabilising the Tokamak RWM that utilises a secondary rotating conducting shell surrounding the plasma and first wall. This scheme was first thought of for the Reversed Field Pinch, but must be re-examined for the Tokamak as the mode involved has different characteristics. It is shown that provided the second wall is suitably positioned, RWM stabilisation of a Tokamak is possible even in the absence of plasma rotation.

I. Introduction

It has long been known that if an ideal plasma is unstable in the absence of a wall, then surrounding the plasma with a finitely conducting wall does not alter the equilibrium stability boundaries.¹ The instability that arises has become known as the resistive wall mode (RWM), and is a generic threat to many toroidal plasma confinement devices. Subsequently, much attention has been given to the effect of bulk plasma rotation on the RWM.² Clearly, if the RWM perturbation travels with the plasma then classical skin effect at the wall would inhibit flux penetration and the wall would appear as highly conducting. On the other hand, if the mode ‘locks’ to the wall despite the plasma rotation then flux penetration would occur and the RWM will continue to grow, albeit initially with a small growth rate. Further, the mode exerts a retarding torque on the plasma, which eventually undergoes a ‘catastrophic’ deceleration while the growth rate suddenly increases.³ This event, which is analogous to the phase changes that occur in a Van der Waal’s gas,⁴ has been tentatively observed experimentally.⁵ So, generation of bulk plasma rotation appears to be an unreliable way of stabilising the RWM although it does have the effect of suppressing the growth rate.

In the context of the Reversed Field Pinch (RFP), where the RWM was first identified,^{6,7} it has been proposed that a secondary rotating conducting shell would stabilise the RWM in that device.⁸ (The suggestion was motivated by the TITAN power plant design that proposed using flowing lithium for the blanket⁹ - it was later shown that a suitable configuration of external sensors and coils could ‘fake’ the existence of such a shell.¹⁰) The simple idea is that the RWM cannot simultaneously lock to both walls and so its behaviour should be strongly affected. In fact it was shown that provided the secondary wall was located inside the ideal marginal radius ($r = r_I$, the radial position at which a perfect wall has to be placed to give the ideal mode zero growth rate), the RWM was stabilised for wall rotations of order the (longest) inverse wall time. Now, in the RFP, the RWM is generally non-resonant (*i.e.* nowhere in the plasma does the pitch of the perturbation equal that of the equilibrium field lines). In this paper we revisit this calculation for the Tokamak, where the relevant RWM is a different mode - the pressure driven toroidal external kink. An essential ingredient of this mode is the presence of

poloidal harmonics which are resonant in the plasma, so the calculation must take this into account. A cylindrical analogue model of this mode was first formulated by Finn,¹¹ and we will use this as a basis. Finn used a cylindrical plasma that was ideally unstable (with no wall) but did possess a resonance. This requires somewhat artificial equilibria but provides a useful qualitative model of the actual Tokamak external kink. Our task is to incorporate a secondary rotating wall into the Finn model.

II. Derivation of the dispersion relation.

The analysis we present relies on the judicious choice of basis functions that will make up the actual mode eigenfunction. In fact we choose basis functions that have a direct physical interpretation. We recall that the problem divides naturally into ideal regions and ‘resistive’ layers (namely the resonance at $r = r_s$ and the static and rotating walls at r_1 and r_2). A second order ODE for the perturbed radial magnetic field, the Newcomb equation,¹² connects the resistive layers and in these layers non-ideal effects have to be taken into account. Figure 1 shows our choice of basis functions generated by the Newcomb equation. The basis function Ψ_1 represents the resistive plasma mode when the stationary wall at r_1 is taken to be a perfect conductor (the boundary conditions are then regularity at the origin $r = 0$ and $\Psi_1(r_1) = 0$). Ψ_2 is, similarly, the resistive plasma mode when the secondary wall is ideal (and the first wall absent). Ψ_3 is the plasma response when there is no wall present at all (so Ψ_3 is identical to Ψ_1 for $0 < r < r_1$ and then has the boundary condition of vanishing as $r \rightarrow \infty$).

Now, to ensure that the system displays the RWM we must have the ideal mode in the absence of a wall unstable and in the Newcomb sense the independent subinterval (r_s, ∞) must be ideally unstable. Further, Newcomb showed that this implies that Ψ_3 must exhibit a zero in this interval. Now we know that this cannot happen in the vacuum region as solutions are $\Psi \propto r^{-m}$ -like (with m the poloidal mode number and using the Tokamak ordering¹³). Therefore, Ψ_3 must exhibit a zero in (r_s, r_1) , as is shown in Fig. 1

The use of these ‘natural’ basis functions ensures not only that the subsequent algebra is minimised, but that we can later relate some of the free parameters that arise to those that occurred in the single wall model.³ To start, we write the eigenfunction as a sum

of the natural basis functions of Fig. 1.

$$\Psi = \Psi_1 + a\Psi_2 + b\Psi_3, \quad (1)$$

where we can choose the coefficient multiplying Ψ_1 to be unity, and can without loss of generality choose one convenient normalisation for each of the $\Psi_{1,2,3}$. In fact, we choose

$$r_1 \frac{d\Psi_1}{dr}(r_1) = -1, \quad (2)$$

$$r_2 \frac{d\Psi_2}{dr}(r_2) = -1, \quad (3)$$

and

$$\Psi_3(r_s) = \Psi_1(r_s). \quad (4)$$

Because we require Eqn. (1) to apply everywhere we must define $\Psi_1(r) \equiv 0, r > r_1, \Psi_2(r) \equiv 0, r > r_2$, and we note that Ψ_1, Ψ_2 have discontinuous derivatives at two points (r_s, r_1) and (r_s, r_2) respectively, while Ψ_3 has a discontinuous derivative only at r_s .

Now at the second wall we assume a ‘thin shell’ response² so that $\Delta'(p)$, the well known jump in the logarithmic derivative of the perturbed radial field¹⁴ across the wall, is simply equal to $p\tau_2$ where we have assumed $\exp(pt)$ dependence and τ_2 is the ‘long’ time constant of the second wall. Accordingly, noting that Ψ_3 and $d\Psi_3/dr$ are continuous through r_2 and using Eqn. (3) we have

$$p\tau_2 = -\frac{a}{b|\Psi_{32}|}, \quad (5)$$

where $\Psi_{32} = \Psi_3(r_2)$. Note that when the second wall is rotating with frequency Ω_2 we simply replace p in Eqn. (5) by $(p - i\Omega_2)$. Similarly, at r_1, Ψ_2, Ψ_3 and their derivatives are again continuous and using Eqn. (2) we find

$$p\tau_1 = \frac{1}{a\Psi_{21} - b|\Psi_{31}|}, \quad (6)$$

The last of the jump conditions occurs at the plasma resistive layer at r_s . For the moment we will not specify the plasma response, but symbolise it as $\Delta'_s(p)$. From first definitions we have

$$\Delta'_s(p) = \frac{r_s \left([\Psi'_1] + a[\Psi'_2] + b[\Psi'_3] \right)}{\Psi_1 + a\Psi_2 + b\Psi_3}, \quad r = r_s, \quad (7)$$

Now recall that we chose $\Psi_{1,2,3}$ to represent the plasma stability properties when respectively, the first wall is perfect, the second wall is perfect (the first being absent), and when there is no wall at all. So first we simply rewrite Eqn. (7) as

$$\Delta'_s(p) = \frac{\Psi_{1s}\Delta'_1 + a\Psi_{2s}\Delta'_2 + b\Psi_{3s}\Delta'_3}{\Psi_{1s} + a\Psi_{2s} + b\Psi_{3s}}, \quad (8)$$

where the $\Delta'_{1,2,3}$ are the stability parameters for the three cases mentioned.

To proceed, we note that for $r \geq r_1$ we have vacuum fields and it is well known that in the Tokamak ordering $\Psi \sim r^m, r^{-m}$ in such regions.¹³ As we require $\Psi_{22} = 0$ and $r_2\Psi'_2(r_2) = -1$ we easily find that

$$\Psi_{21} = \frac{r_2^{2m} - r_1^{2m}}{2mr_1^m r_2^m}. \quad (9)$$

For $r \geq r_1$, Ψ_3 can only be r^{-m} -like, and it follows that

$$|\Psi_{32}| = \left(\frac{r_1}{r_2}\right)^m |\Psi_{31}|. \quad (10)$$

Putting Eqns. (9,10) into Eqns. (5,6) we can solve for a and get b in terms of $|\Psi_{31}|$

$$a = \frac{2mr_1^m r_2^m \tau_2}{[(r_2^{2m} - r_1^{2m})p\tau_2 + 2mr_2^{2m}]\tau_1}, \quad (11)$$

$$b = -\frac{ar_2^m}{p\tau_2 r_1^m |\Psi_{31}|}. \quad (12)$$

By design we have that $\Psi_{3s} = \Psi_{1s}$ and so Eqn. (8) contains the unknown fluxes Ψ_{2s} and Ψ_{1s} , only in the combination Ψ_{2s}/Ψ_{1s} . To solve for this combination we now use a generic property of any second order ODE such as the Newcomb equation, namely that it simply converts the values of Ψ and Ψ' at one radial station to their values at another station via a real linear transformation; in particular we can immediately write

$$\Psi_{1s} = c\Psi_{11} + d\Psi'_{11}, \quad (13)$$

$$\Psi_{2s} = c\Psi_{21} + d\Psi'_{21}, \quad (14)$$

$$\Psi_{3s} = c\Psi_{31} + d\Psi'_{31}, \quad (15)$$

for some real numbers c, d that are functionals of the mode numbers and the equilibrium fields in between r_s and r_1 . The right hand sides of Eqns. (13) and (15) are $-d/r_1$ and

$-c|\Psi_{31}| + md|\Psi_{31}|/r_1$, respectively, while the RHS of Eqn. (14) is known because, as remarked above, we can easily solve for Ψ_2 in $r_1 < r < r_2$. So, Eqns. (13 - 15) constitute the required linear algebra problem which will enable us to solve for Ψ_{2s}/Ψ_{1s} . We find

$$\frac{\Psi_{2s}}{\Psi_{1s}} = \frac{1}{\sqrt{Y}} \left(Y - \frac{1}{X|\Psi_{31}|} \right) \quad (16)$$

where

$$X = \frac{2m}{1-Y}, \quad Y = \left(\frac{r_1}{r_2} \right)^{2m}.$$

Note that using Eqns. (11), (12) and (16), and the fact that $\Psi_{1s} = \Psi_{3s}$, the dispersion relation Eqn. (8) now contains only one unknown flux, namely $|\Psi_{31}|$. This final unknown can be solved for when we realise that Ψ_1, Ψ_2 and Ψ_3 are not independent in the plasma region (again because the governing Newcomb equation is of second order). Accordingly we can write

$$\Psi_2 = e\Psi_1 + f\Psi_3, \quad (17)$$

for some real constants e and f . Applying this relationship at $r = r_s$ gives

$$\Psi_{2s} = (e + f)\Psi_{1s}, \quad (18)$$

while differentiating Eqn. (17) and evaluating at either side of $r = r_s$ gives

$$\Delta'_2 = \frac{e\Delta'_1 + f\Delta'_3}{(e + f)}. \quad (19)$$

Applying Eqn. (17) directly at $r = r_1$ gives

$$\Psi_{21} = -f|\Psi_{31}|. \quad (20)$$

Now Eqns. (9), (18), (19), and (20) constitute another linear algebra problem from which we can deduce $|\Psi_{31}|$. In fact,

$$|\Psi_{31}| = \frac{1}{XY} \frac{(\Delta'_2 - \Delta'_3)}{(\Delta'_2 - \Delta'_1)}. \quad (21)$$

So now, using Eqns. (11), (12), (16) and (21) together with $\Psi_{1s} = \Psi_{3s}$, we find the basic dispersion relation

$$\Delta'_s(p) = \frac{(\Delta'_2 - \Delta'_1)\Delta'_3 X^2 Y + (\Delta'_3 - \Delta'_1)\Delta'_2 X Y p \tau_2 + (\Delta'_3 - \Delta'_2)\Delta'_1 (X + p \tau_2) p \tau_1}{(\Delta'_2 - \Delta'_1) X^2 Y + (\Delta'_3 - \Delta'_1) X Y p \tau_2 + (\Delta'_3 - \Delta'_2) (X + p \tau_2) p \tau_1} \quad (22)$$

To ensure that we are investigating a RWM, we must have a plasma equilibrium that is ideal-MHD unstable in the absence of walls.^{1,2} This means that Δ'_3 must display an ideal, inertial response at the resonance r_s *i.e.* $\Delta' = -1/(p\tau_A)$ with τ_A the Alfvén time.¹⁵ So if we write $\Delta'_3 = -1/\epsilon$ then positive ϵ gives the (τ_A) normalised growth rate of the ideal mode in the absence of a wall. (The parameter ϵ appeared, with the same interpretation, in the earlier work on the single wall model.³) We also follow the notation of Ref. 3 by writing $\Delta'_2 = -\delta$, so for conventional tearing modes, say, positive δ would imply stability.¹⁴ Using this notation the dispersion relation (22) can be rewritten

$$\Delta'_s(p) = \frac{X^2Y (\delta + \Delta'_3) - \delta (1 + \epsilon\Delta'_3) (X + p\tau_2) p\tau_1 + XY\Delta'_3 (1 - \epsilon\delta) p\tau_2}{-\epsilon X^2Y (\delta + \Delta'_3) + (1 + \epsilon\Delta'_3) (X + p\tau_2) p\tau_1 + XY (1 - \epsilon\delta) p\tau_2}. \quad (23)$$

III. Analysis of the dispersion relation

We choose the actual layer response to be ‘visco-resistive’¹⁶

$$\Delta'_s = p\tau_{VR}, \quad (24)$$

where $\tau_{VR} \sim \tau_A^{1/3} \tau_R^{5/6} / \tau_V^{1/6}$ and τ_R, τ_V are, respectively, characteristic layer resistive and viscous times. This response is appropriate to most tokamak plasmas.¹⁶ We recall that this choice of layer response is ‘pessimistic’ in that in the case of the single wall problem, a visco-resistive layer response eradicated all RWM stability windows.³ With the choice of Eqn. (24) as the layer response the dispersion relation Eqn. (23) is a complex cubic (bearing in mind that we Doppler shift $p\tau_{VR} \rightarrow (p - i\Omega_{pl})\tau_{VR}$ and $p\tau_2 \rightarrow (p - i\Omega_2)\tau_2$ to simulate plasma and second wall rotation). We shall mainly investigate Eqn. (23) numerically, but before that there is one analytic observation we can make.

If the RWM is to be stabilised by some combination of Ω_{pl} and Ω_2 then its growth rate must at some stage achieve marginality, *i.e.* $p = i\omega$ for real ω . Inserting this into (23) and taking real and imaginary parts we can take the limit $\Omega_2 \rightarrow \infty$ to find that at marginality we must have

$$\Omega_{pl}^2 = \left(\frac{\Delta'_2}{\delta} \right) \left[\frac{(\epsilon\delta - 1) \tau_{VR} XY^2 - (\epsilon\Delta'_2 + 1) \delta \tau_1}{(\epsilon\Delta'_2 + 1) \tau_1 \tau_{VR}} \right]^2. \quad (25)$$

Equation (25) indicates immediately that the ‘topology’ of the marginal curve in Ω_2, Ω_{pl} space will be strongly influenced by the relative signs of Δ'_2 and δ : if they are the same

sign we have real solutions for Ω_{pl} and if they are not the same sign there are none. To investigate this, the cubic (23) was solved, and contours of equal growth rate plotted in Ω_2, Ω_{pl} space.

Now, Δ'_2 and δ are important parameters because, between them, they implicitly determine where the two walls are positioned radially with respect to two naturally occurring radii, r_I and r_R . These are the radii that a perfect wall has to be placed to make the ideal and resistive modes marginally stable, respectively. We now construct illustrative examples that enumerate the various possibilities.

(1) We start by considering the case where the second wall is *outside* r_I . This means that the ideal mode is unstable even if the second wall is perfect. This in turn means that Δ'_2 will be large and negative (as the ideal marginal point r_I goes from just inside r_2 to just outside then Δ'_2 goes from large positive to large negative). In Fig. 2 we plot contours of equal growth rate for such a case ($\Delta'_2 = -100$, and ‘typical’ values for the rest of the parameters $\epsilon = 0.1, \delta = 1, \tau_1 = \tau_2 = \tau_{VR} = 1, r_1 = 1.2, r_2 = 1.4, m = 2$). In this and the following figures the dashed contours represent positive (unstable) growth rates and the solid contours negative (stable) growth rates. We see immediately that all growth rates are positive, and that stabilisation of the RWM is impossible in this case for any combination of Ω_{pl} and Ω_2 (notated OMEGA_PL and OMEGA_2 in the figures). This is not surprising as the ideal mode is not really a RWM, but an ideal mode ‘in its own right’ as $r_2 > r_I$. The symmetry evident in the figure is a straightforward consequence of the model geometry.

(2) Now let us reverse this condition and move r_2 inside r_I . Δ'_2 will now be generically large and positive. Figure 3 shows the results for this case ($\Delta'_2 = 5$, all other parameters the same as Fig. 2). Note the appearance of stable regions. However, access to each of the stable regions requires a sufficient amount of plasma rotation. As the second wall is moved further towards the plasma then Δ'_2 drops and so do the amounts of Ω_2, Ω_{pl} required for stabilisation.

(3) As the wall is moved further in then the next radius of importance it encounters is

r_R , the marginal radius of the resistive mode. At this point, of course, $\Delta'_2 = 0$. Figure 4 shows the case where r_2 has just moved inside r_R and $\Delta'_2 = -0.3$ (all other parameters the same as in Figs. 2 and 3). We see there has been a topology change due to the change of sign of Δ'_2 , and now it is possible to access a stable region with *no* plasma rotation present.

(4) As the second wall is now moved towards r_1 , although RWM stabilisation is still possible with $\Omega_{pl} = 0$ it becomes increasingly more difficult in terms of the amplitude of Ω_2 required. In fact, in the limit of $r_2 \rightarrow r_1$ inspection of Eqn. (23) shows that in the limit the two walls merge electromagnetically and the combination is ‘seen’ by the plasma as a single wall with time constant $\tau_1 + \tau_2$. The system is then the single wall problem of Ref. 3. Figure 5 shows the case with $\delta = 1, \Delta'_2 = -0.995, r_2 = 1.204$ (to accord with the limit $r_2 \rightarrow r_1$), all other parameters as above.

(5) Lastly we can imagine a case where $r_R < r_1$, *i.e.* the resistive mode is unstable even were the first wall perfect. Figure 6 shows the case $\delta = -0.01, \Delta'_2 = 0.5$, all other parameters as in Fig. 2. Stable regions have practically disappeared. Again, this is not surprising as, similar to the case of Fig. 2, the active mode is not truly a RWM, but a resistive mode ‘in its own right’.

IV. Conclusions

It appears that relying on plasma rotation *per se.* to stabilise the RWM is not a realistic proposal. We have examined the scheme of utilising a secondary rotating wall to stabilise the RWM in a Tokamak. A model that simulates the actual toroidal nature of the Tokamak RWM (generated by the ideal pressure driven external kink mode) has been used. Results depend strongly on the position of the second wall (r_2) with respect to the ideal and resistive marginal radii r_I and r_R (these are, respectively, the radii at which a perfect wall must be placed to make the ideal and resistive modes marginally stable). RWM stabilisation is impossible if $r_2 > r_I$, but possible with finite

plasma rotation if $r_R < r_2 < r_I$. Further, the rotation rates required are ‘slow’ in the sense that they are of order the inverse wall time of the least conducting wall. If $r_2 < r_R$ then stabilisation is possible even in the absence of plasma rotation. (However, as r_2 approaches r_1 stabilisation becomes increasingly more difficult, and there is an optimisation problem.)

This scheme was first considered for the RFP, where the TITAN power plant design used a flowing lithium blanket.^{8,9} However, it was later realised that a secondary rotating wall could be ‘faked’ by a suitable array of external sensors and active coils.¹⁰ What is more, such a wall is projectable and need not reside at the actual location of the coils, a property which may be required in power plant designs.¹⁷ Reference 17 also stated that the gain, bandwidth, current and total power requirements of the feedback system could be estimated as less than a hundred, a few Hz, a few tens of kA and a few MW respectively. These requirements are within the scope of present technology. This scheme, together with that of the ‘intelligent’ shell¹⁸ (which seeks to directly simulate an ideal wall with external sensors and coils), appear to form a useful basis for stabilising the RWM in fusion Tokamak power plants.

Acknowledgments.

We thank A. Caloutsis for assistance in producing the stability figures. This work was funded jointly by the UK DTI and EURATOM.

References

- ¹D. Pfirsch and H. Tasso, Nucl. Fusion **11**, 259 (1971).
- ²C. G. Gimblett, Nucl. Fusion **26**, 617 (1986).
- ³C. G. Gimblett and R. J. Hastie, Phys. Plasmas **7**, 258 (2000).
- ⁴R. S. Peckover and C. G. Gimblett, Bulletin of the Institute of Mathematics and its Applications **17**, 73 (1981).
- ⁵E. J. Strait, Personal Communication (1999).
- ⁶B. Alper, M. K. Bevir, H. A. B. Bodin, C. A. Bunting, P. G. Carolan, J. Cunnane, D. E. Evans, C. G. Gimblett, R. J. Hayden, T. C. Hender, A. Lazaros, R. W. Moses, A. A. Newton, P. G. Noonan, R. Paccagnella, A. Patel, H. Y. W. Tsui, and P. D. Wilcock, Plasma Phys. Control. Fusion **31**, 205 (1989).
- ⁷P. Greene and S. Robertson, Phys. Fluids B **5**, 556 (1993).
- ⁸C. G. Gimblett, Plasma Phys. Contr. Fusion **31**, 2183 (1989).
- ⁹'The TITAN Reversed-Field Pinch Fusion Reactor Study', Scoping Phase Report, UCLA-PPG-1100, (1987).
- ¹⁰T. H. Jensen and R. Fitzpatrick, Phys. Plasmas **3**, 2641 (1996).
- ¹¹(i) J. M. Finn, Phys. Plasmas **2**, 198 (1995).
(ii) J. M. Finn, Phys. Plasmas **2**, 3782 (1995).
- ¹²W. A. Newcomb, Annals of Physics, **10**, 232 (1960).
- ¹³J. A. Wesson, *Tokamaks*, (Clarendon, Oxford, 1987).
- ¹⁴H. P. Furth, J. Killeen, and M. N. Rosenbluth, Phys. Fluids **6**, 459 (1963).
- ¹⁵G. Ara, B. Basu, B. Coppi, C. Laval, M. N. Rosenbluth and B. V. Waddell, Annals of Physics, **112**, 443 (1978).
- ¹⁶R. Fitzpatrick, Nucl. Fusion **33**, 1049 (1993).

¹⁷R. Fitzpatrick, Phys. Plasmas **4**, 2519 (1997).

¹⁸C. M. Bishop, Plasma Phys. Contr. Fusion **31**, 1179 (1989).

FIGURE CAPTIONS

Figure 1: Basis functions used in the RWM analysis.

Figure 2: The second rotating wall is outside the ideal marginal radius and stabilisation of the 'RWM' is impossible.

Figure 3: The second rotating wall is inside the ideal marginal point and stabilisation is possible providing there is sufficient plasma rotation.

Figure 4: The second rotating wall is inside the resistive marginal point and RWM stabilisation is possible with no plasma rotation.

Figure 5: As the second rotating wall approaches the first, RWM stabilisation becomes increasingly more difficult in terms of the amplitude of Ω_2 required.

Figure 6: The marginal radius for the resistive mode is inside r_1 and stable regions have practically disappeared.

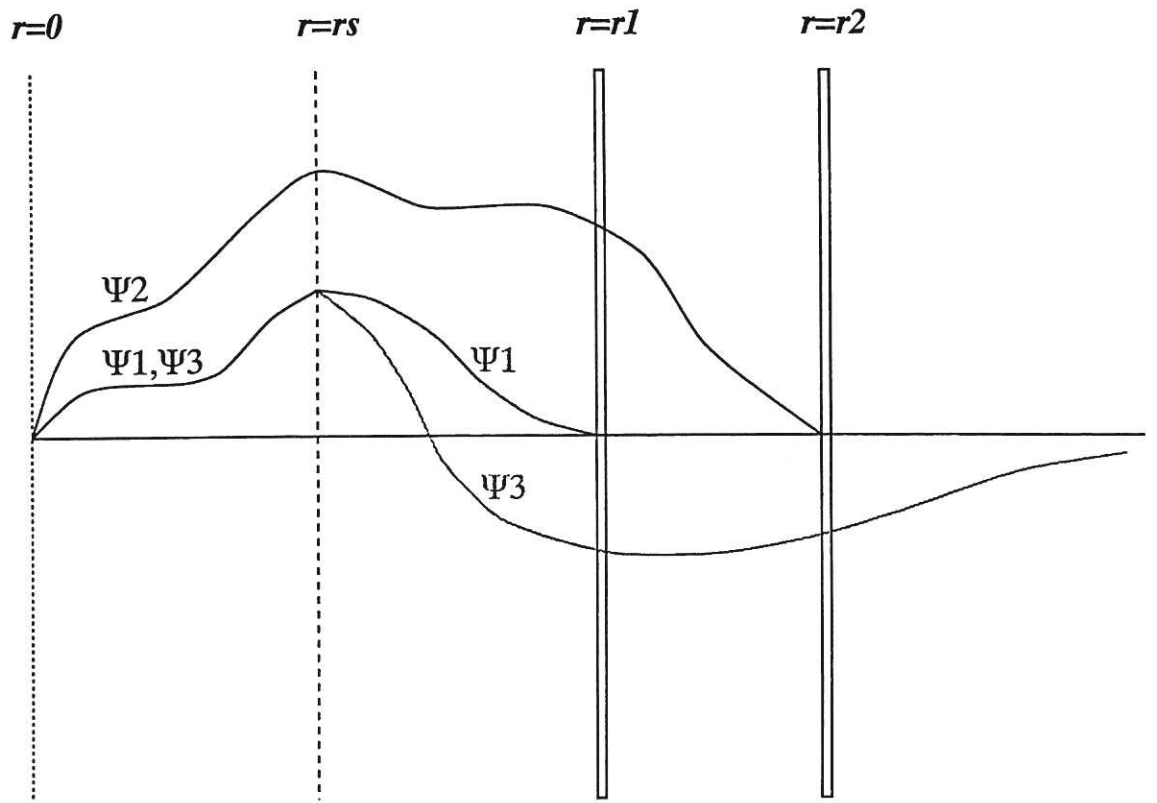


Figure 1: Basis functions used in the RWM analysis.

GROWTH RATE CONTOURS

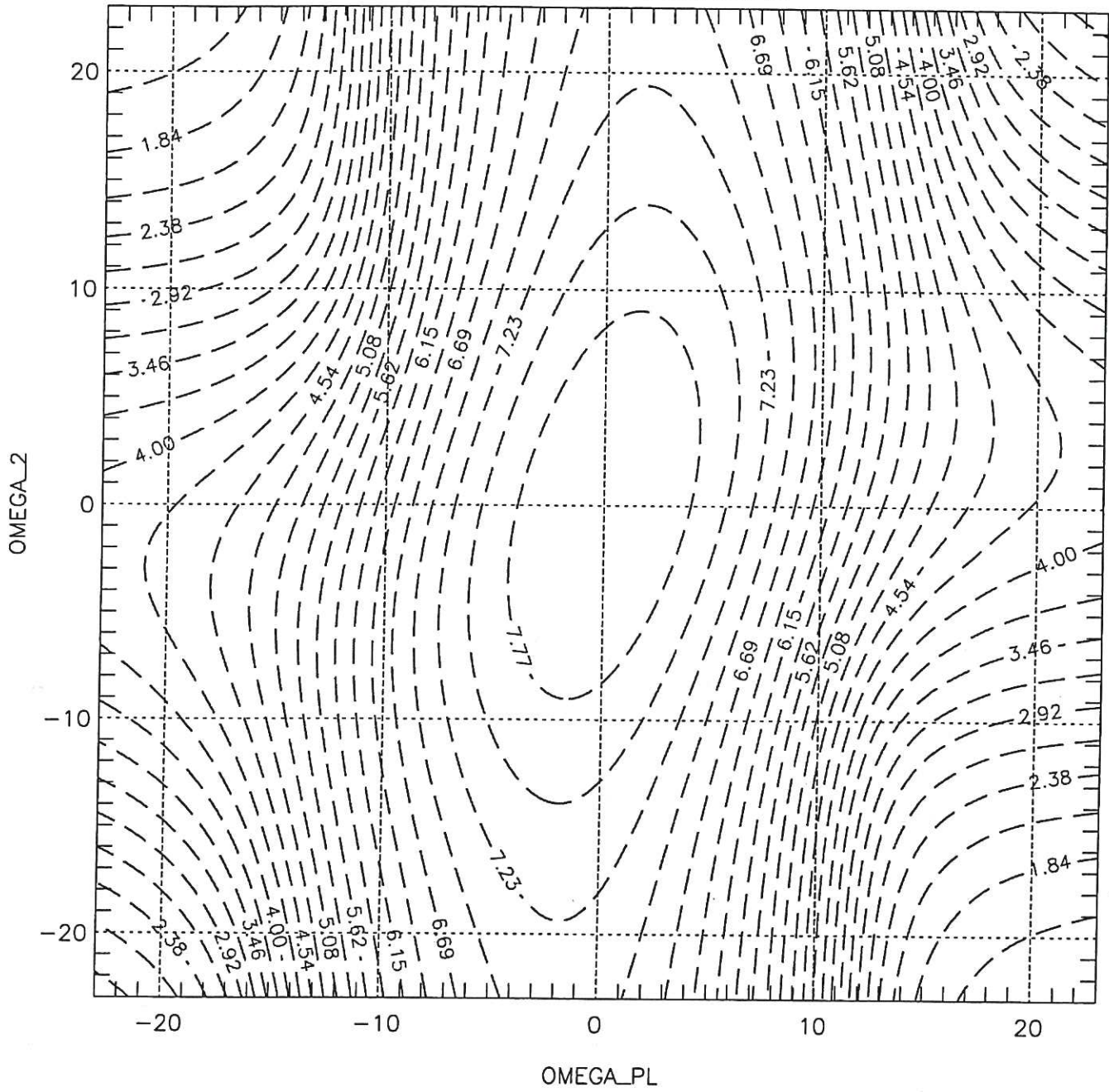


Figure 2: The second rotating wall is outside the ideal marginal radius and stabilisation of the 'RWM' is impossible.

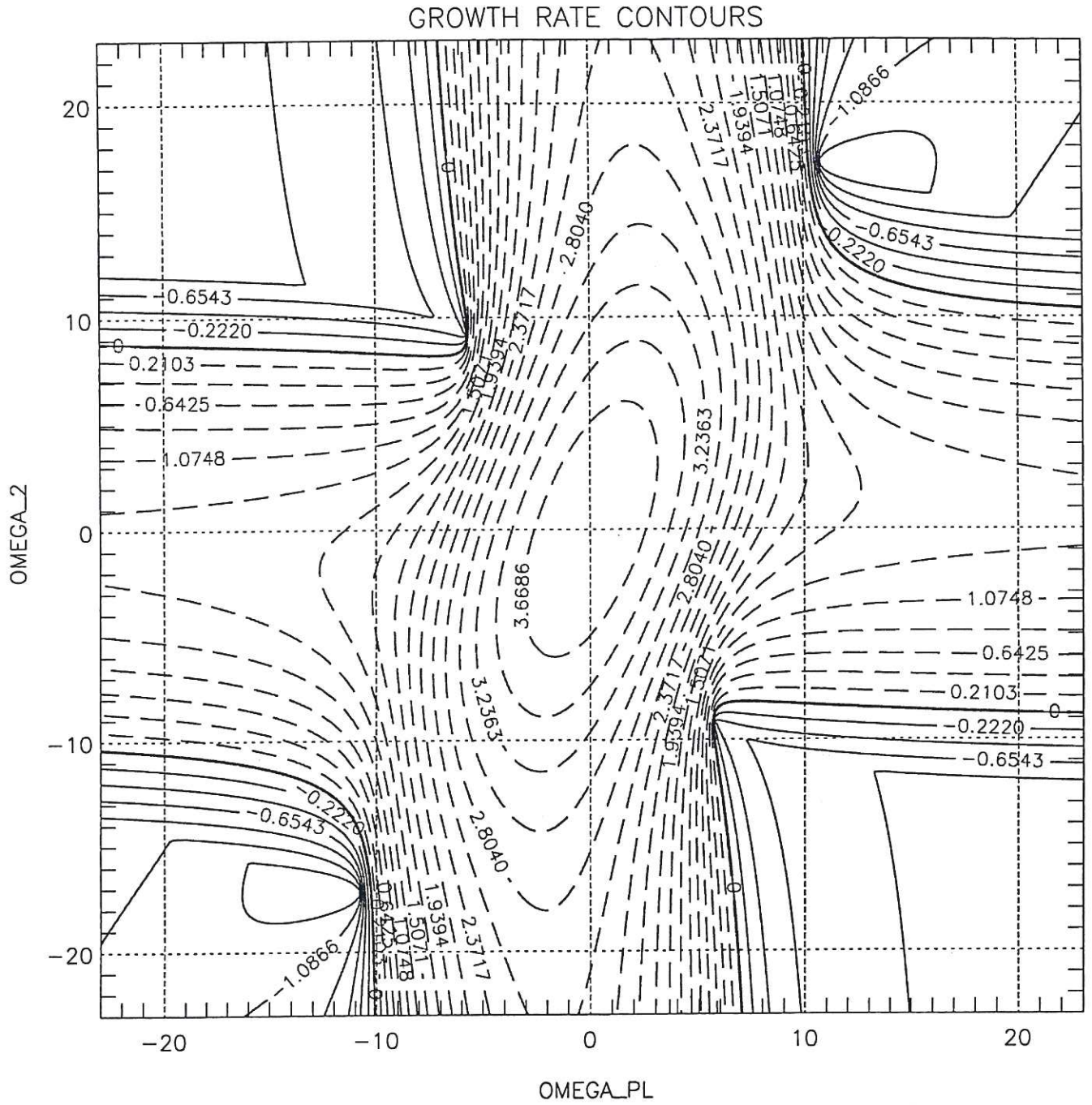


Figure 3: The second rotating wall is inside the ideal marginal point and stabilisation is possible providing there is sufficient plasma rotation.

GROWTH RATE CONTOURS

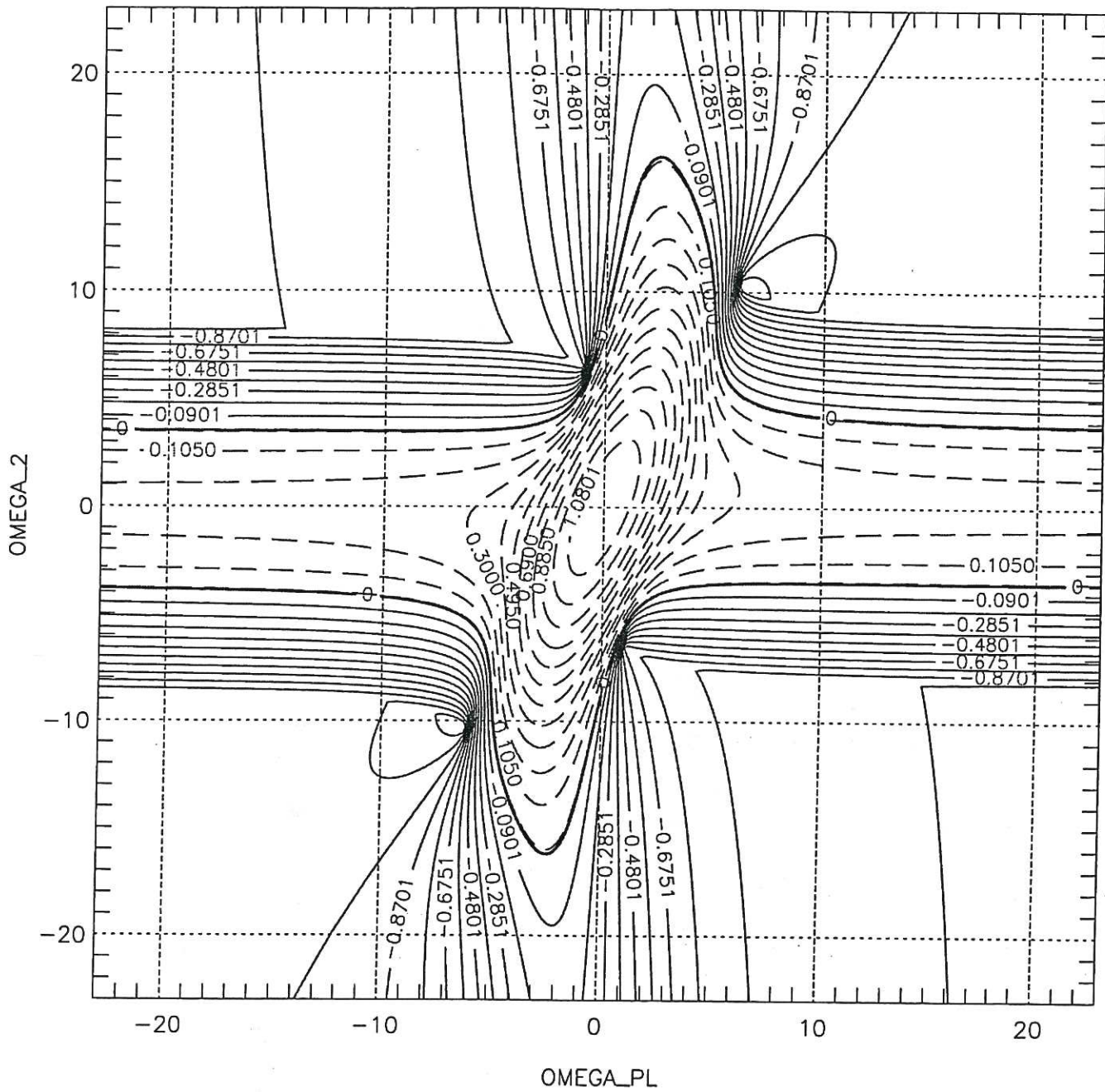


Figure 4: The second rotating wall is inside the resistive marginal point and RWM stabilisation is possible with no plasma rotation.

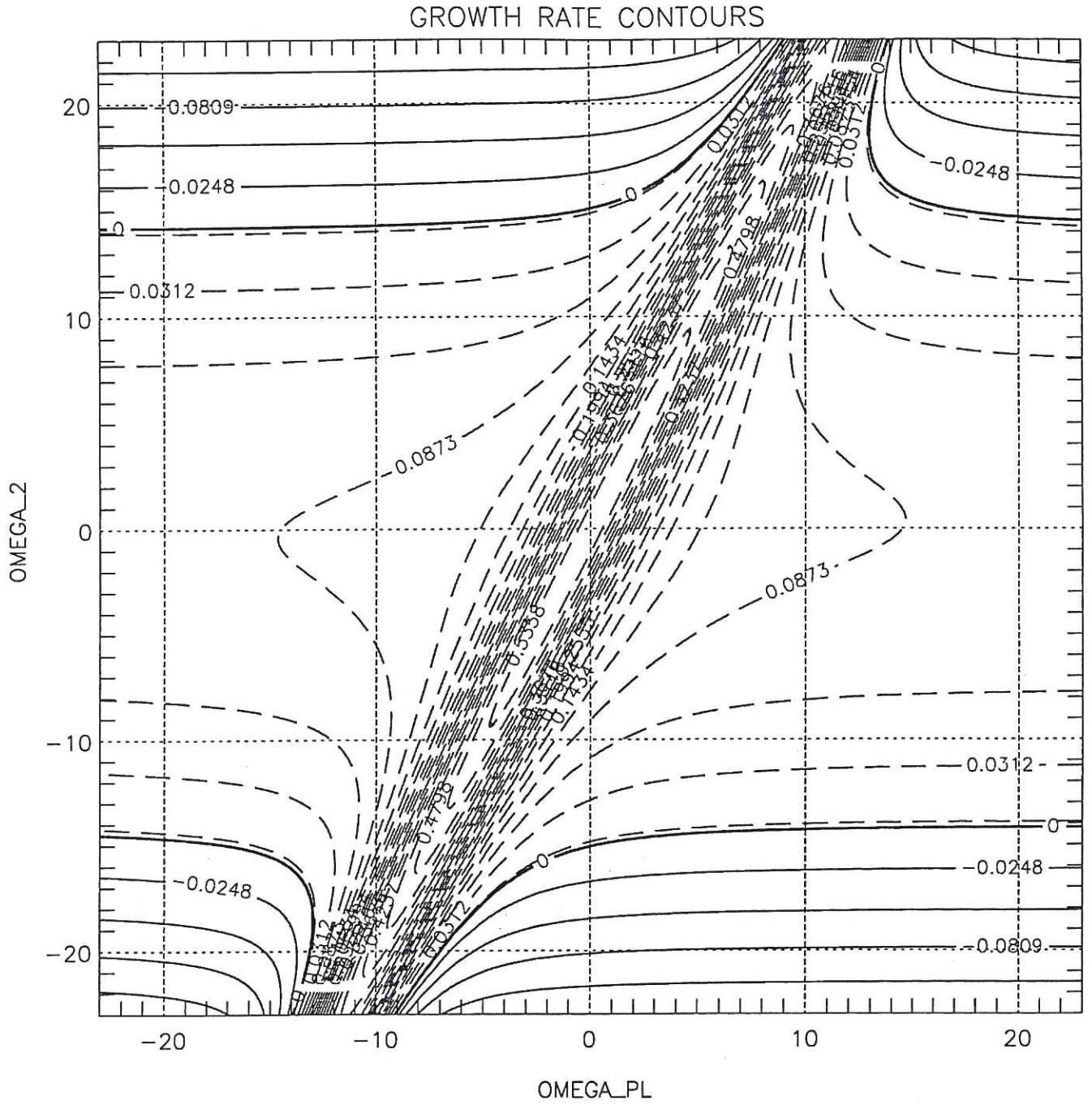


Figure 5: As the second rotating wall approaches the first, RWM stabilisation becomes increasingly more difficult in terms of the amplitude of Ω_2 required.

GROWTH RATE CONTOURS

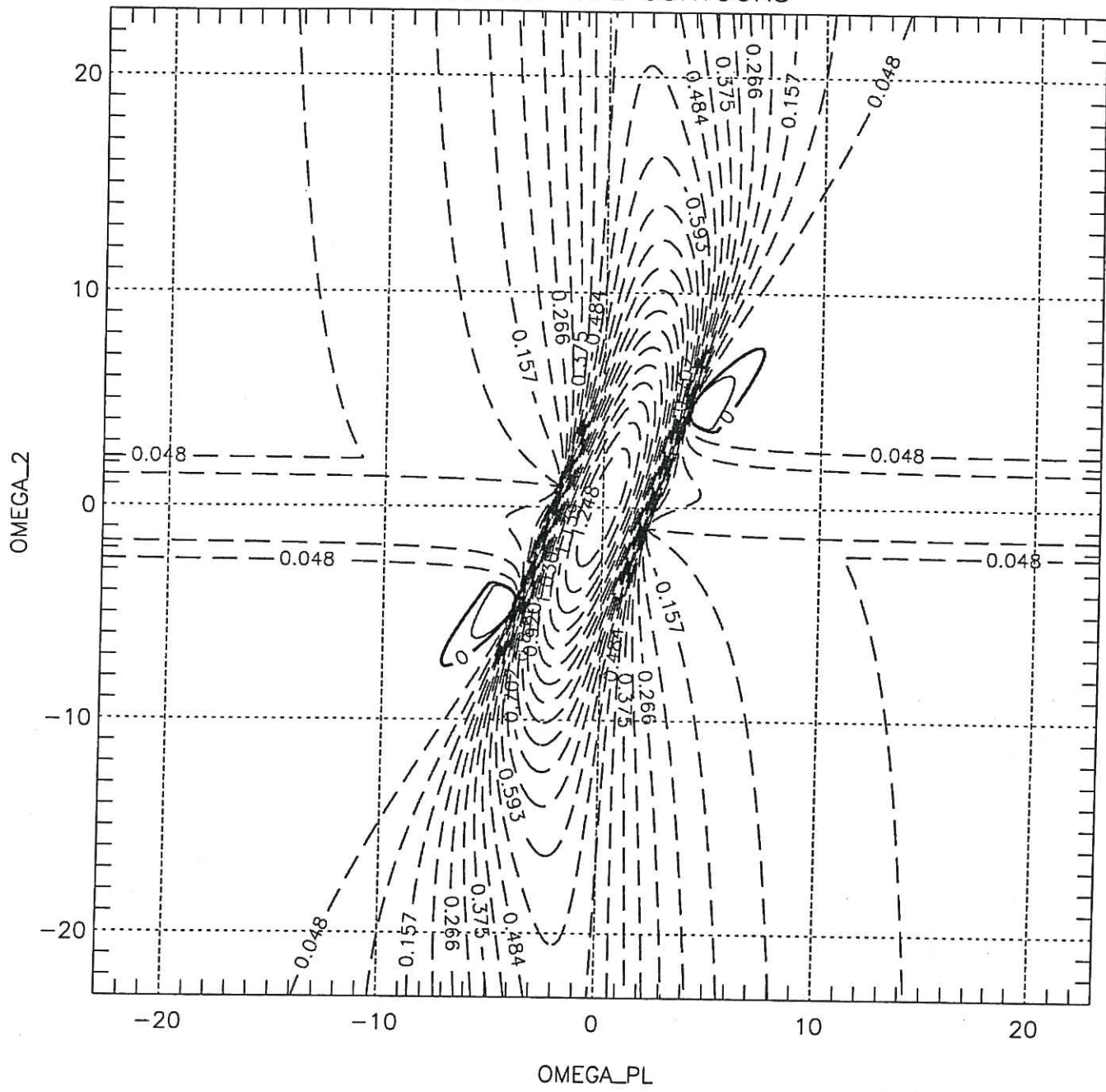


Figure 6: The marginal radius for the resistive mode is inside r_1 and stable regions have practically disappeared.

